ACÚSTICA 98

RECENT ADVANCES IN ACOUSTICS AND VIBRATION

Malcolm J. Crocker
Department of Mechanical Engineering
Auburn University, AL 36849, USA
Tel: (1) 334-844-3310; Fax: (1) 334-844-3306
e-mail: mcrocker@eng.auburn.edu

SUMMARY

In recent years there have been rapid advances in digital computers, the miniaturization of electronic circuits and the development of new materials. In the acoustics and vibration fields these advances have led to a continual increase in computational power and speed, improved acoustics and vibration transducers and instrumentation and better measurement techniques. Improved computers have allowed the development of a host of computer programs and increasing numbers have become available as commercial acoustics and vibration software. The development of numerical calculation schemes such as the finite element method (FEM) and the boundary element method (BEM) which have led to much improved predictive capabilities in many fields. However, advances have been in many other areas of acoustics as well and not confined just to such numerical prediction schemes. As examples, a few of these will be concisely summarized including: increased knowledge of and use of FEM and BEM, Computational Aeroacoustics, Sonochemistry, Thermoacoustic Engines, Active Noise and Vibration Control, Sound Intensity Measurements and their uses, Techniques of Speech Coding and Recognition of Speech, Ultrasonics in Medical Diagnostics, and Cochlear Mechanics.

INTRODUCTION

The development of the digital computer in the late 1950's enabled rapid calculations and analytical solutions of problems that were previously insoluble because of the enormous amount of calculations and time and manpower needed for their solution. The continuing development has also brought lower costs and miniaturization of components and the late 1970's saw the development of the desktop and portable computers that put computing power into the hands of increasing numbers of scientists. Some very visible results have been the development of Finite Element Analysis (FEM) and the Boundary Element Method (BEM) that can solve complicated acoustics and vibration problems and of increasing numbers of software programs that can run on mainframe and on desktop and portable computers. Digital computers have also increasingly been built into instrumentation and analysis equipment enabling more sophisticated experimentation in acoustics and vibration and more rapid and detailed analysis of the results. The development of piezoelectric materials has also led to advances in the design of acoustics and vibration transducers. These and other developments have had a synergistic effect and have enabled or aided advances in several fields of acoustics and vibration. Some of these are outlined in the following.

NUMERICAL APPROACHES: FINITE ELEMENTS AND BOUNDARY ELEMENTS

In cases where the geometry of a vibrating structure or an acoustic space is complicated and where lumped element or modal approaches cannot be used, then it is necessary to use numerical approaches. In the late 1960's with the advent of powerful digital computers, FEM approaches were first used to analyze static and then dynamic (vibration) structural problems. [1] Later FEM was used with acoustics problems. In the FEM approach the fluid volume is divided into a number of small fluid elements (usually rectangular or triangular) and the equations of motion are solved for the elements, ensuring that the sound pressure and volume velocity

are continuous at the node points where the elements are joined. The FEM has been widely used to study the acoustical performance of elements in automobile cabins and muffler systems and aircraft problems. [2,3]. Such FEM programmes are now widely available from commercial software companies. Craggs has given a good recent review of the use of FEM in acoustics. [2] Figure 1 shows a cavity representing that of an automobile interior. In a recent study thirty 32-node elements were used resulting in a system with 378 degrees of freedom. A comparison of predicted and measured natural frequencies is given in Table 1.

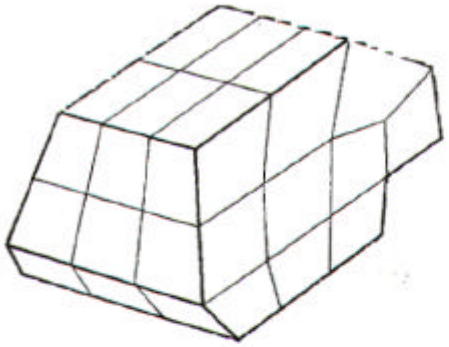

FIG 1 Acoustic finite element grid for a model car enclosure Assembly is of the 32-node isoparametric elements.

Table 1 Natural Frequencies of Irregular Cavity

Mode	Finite Element Simulation	Measured Frequency
100	140.8	154.6
001	160.3	168.2
010	208.9	220.2
200	243.3	251.0
101	267.8	281.8
201	288.8	301.8
110	299.9	312.2
110	299.9	312.2
002	313.4	323.8
102	353.2	355.4
111	347.6	366.6
020	371.3	378.2

The boundary element method was developed a little later than the FEM. In the BEM approach the elements are described on the boundary surface only, which reduces the computational dimensions of the problem by one. This correspondingly produces a smaller system of equations than the FEM and thus saves computational time considerably because of the use of a surface mesh instead of a volume mesh. For sound propagation problems involving the radiation of sound to infinity, the BEM is more suitable because the radiation condition at infinity can be easily satisfied with the BEM, unlike with the FEM. However, the FEM is better suited than the BEM for the determination of the natural frequencies and mode shapes of cavities. Seybert and Yu have discussed the use of BEM in acoustics problems in a recent review. [4]
Figure 2 shows a boundary element mesh model for the sound radiated from a tire touching the hard reflecting ground plane together with the contours of the sound pressure levels radiated by the tire at 100 Hz. [4] In the last decade FEM and BEM commercial software have become widely available.

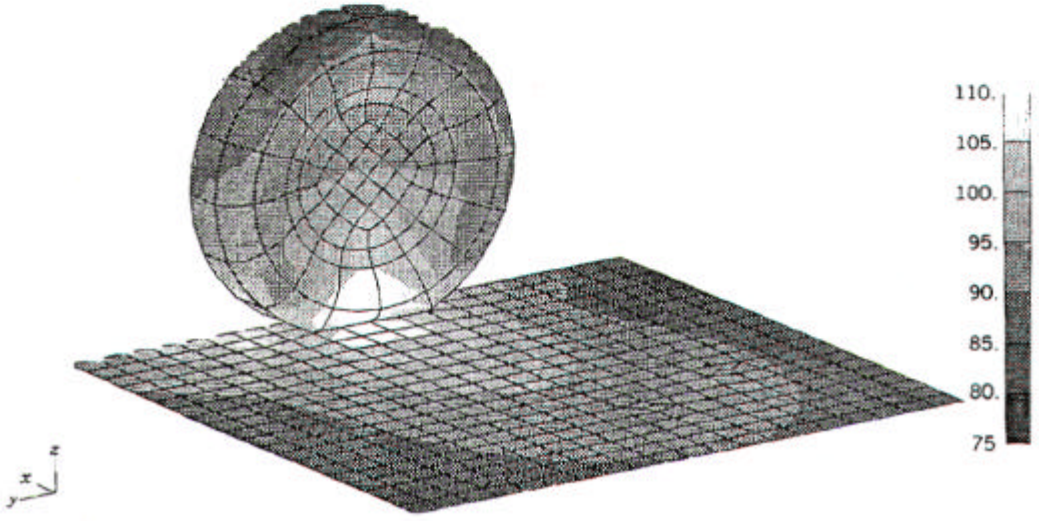

FIG 2 The SPL contour plot of tire radiation at 100 Hz.

Figure 3 shows a boundary element mesh used for a simple expansion chamber muffler. After the mesh shown is created by the user (with element size no larger than a certain fraction of the acoustic wavelength) the boundary condition information at every node is supplied to the BEM. The BEM is used to calculate the sound pressure on the inner surface of the cavity as well as at field points inside the cavity. The transmission loss (TL) both calculated using the BEM (solid line) and measured experimentally (triangles) is shown in Fig. 4. [7] The BEM results were obtained by specifying the velocity at all of the node points to be zero (since the muffler casing was assumed to be rigid) except for the nodes at the inlet and exit of the muffler. At the inlet the velocity was specified to be unity and at the outlet the boundary condition was that the acoustic impedance was equal to the characteristic impedance of the medium. Figure 3 shows the contours of equal sound pressure level at 2900 Hz, a frequency at which the TL is approximately zero (see Fig. 4). Figure 3 shows that there is a cross mode at this frequency resulting in the poor TL.

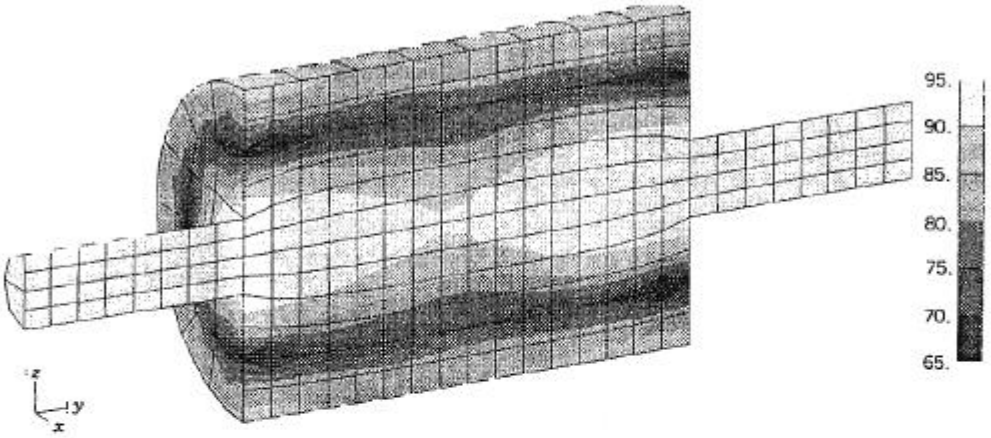

FIG 3 The SPL contour plot for the expansion chamber muffler at 2900 Hz

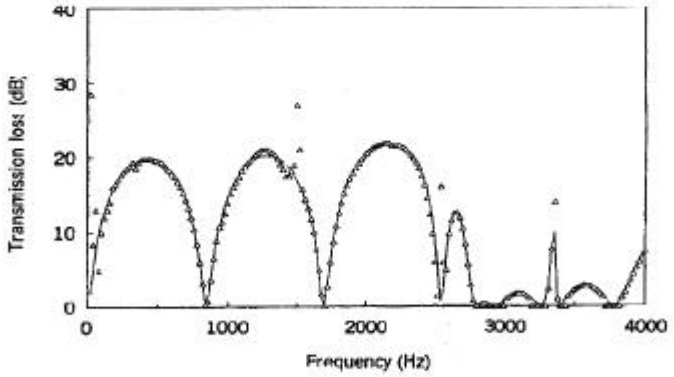

FIG 4 The TL for a simple expansion chamber muffler: solid line, BEM; symbols, experiment.

Recently the FEM and BEM approaches have been combined to obtain a powerful tool for the solution of vibro-acoustic problems. This approach is sometimes known as BFEM. [5] With BFEM, normally FEM is used for modeling the vibration response of a structure and BEM for modeling the sound radiation into the fluid.

COMPUTATIONAL ACOUSTICS

Although both classical modal approaches and the FEM and BEM are useful in solving a variety of complicated acoustic problems it is difficult to include the effects of either mean or unsteady fluid flow in these approaches. Recently digital computers have also become useful in predicting sound propagation in flowing fluid media. [6]

There are several possible approaches. In one approach the Navier Stokes equations for flow are used in a time marching scheme to obtain a steady state solution. The unknown variables are the fluid density, fluid velocity components, and the total fluid energy. The components of the viscous stress tensor and the heat flux vector are computed from flow variables. [7] In order to derive the equations that govern the acoustic disturbances in the flow, the unknown fluid variables are decomposed into mean or steady flow components and acoustic perturbation components. By subtracting the equation governing the mean flow from the full fluid dynamic equation, a set of hyperbolic nonlinear equations governing acoustic disturbances in a viscous compressible flow is obtained. There are no exact analytical solutions to these equations and it is necessary to linearize them. The nonlinear equations are linearized by neglecting products of acoustic variables. In order to solve the equations numerically, a consistent set of boundary conditions needs to be prescribed. Boundary conditions for flow duct acoustics have been formalized for some ideal cases, such as hard-walled ducts where it can be assumed that the normal velocity at the wall is zero. The inflow and outflow and the wall boundary conditions need to be considered separately. Computational acoustics is carried out in the time domain. This causes complications with the boundary conditions at the walls of absorbing ducts (where the sound pressure and velocity must be prescribed separately and impedance concepts cannot be used because the formulation is necessarily in the time domain.) Figure 5 shows an example of one of a family of experimental interferograms taken by Zhang and Edwards in experiments on a cavity flow at supersonic speeds. Figure 6 shows one of a family of numerical interferograms obtained by Zhang et al. [6] The figures show contours of equal fluid density. The agreement is seen to be qualitatively good. Detailed quantitative agreement has also been shown. [6]

FIG 5 Experimental Interferogram showing shear layer impingement M∞=1.5, Zhang and Edwards

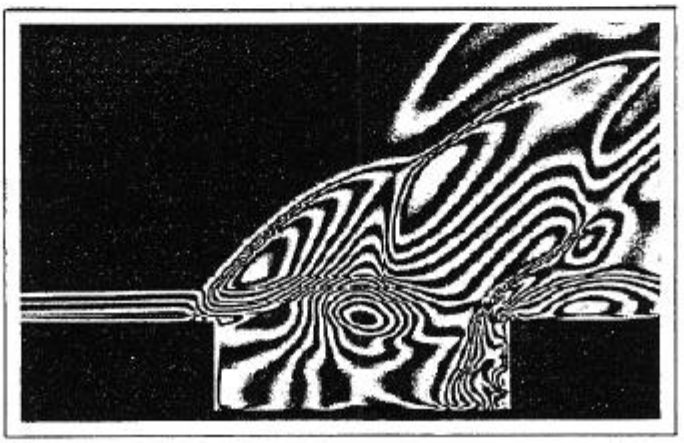

FIG 6 Numerical Interferogram M∞=1.5, showing shear layer impingement, Zhang et al.

ULTRASONICS, SONOCHEMISTRY AND SONOLUMINESCENCE

During the ultrasonic irradiation of liquids, high energy chemical reactions can occur. The chemical reactions that occur do not, however, come from the direct interaction between the ultrasound waves and the chemical molecules. The speed of sound in most liquids is of the order of 1500 m/s and ultrasonic frequencies span the range of about 15 kilohertz to tens of megahertz resulting in acoustic wavelengths of the order of 10 to 10^{-4} cm. These are not molecular dimensions. Instead when ultrasound passes through a liquid the bubbles can form, grow rapidly and then implode as shown in Fig 7.

Ultrasound consists of expansion and compression waves. If the sound waves are intense enough, the expansion waves can cause cavities (bubbles) to occur. Then the compression wave compresses the bubble. The next expansion wave re-expands it and so on. The bubble oscillates at the frequency of the sound field and can grow through various mechanisms including rectified diffusion. With this mechanism the surface area after expansion is greater than the surface area after compression and so the bubble grows. The oscillating bubble tends to grow until it reaches a resonant size and condition determined by the sound field. When the bubble is at resonance it is coupled well to the sound field and can readily absorb energy even in a single cycle. After such growth it is no longer coupled well to the sound field. Then the surface tension together with the next compression wave causes an implosive collapse of he bubble in a very short time. During the collapse a shock wave can exist in the bubble gas and very rapid (and almost adiabatic) heating occurs causing enormous localized temperatures and pressures. Local hot spots occur in the liquid and are responsible for rapid chemical changes (sonochemical) and light emission (sonoluminescence).

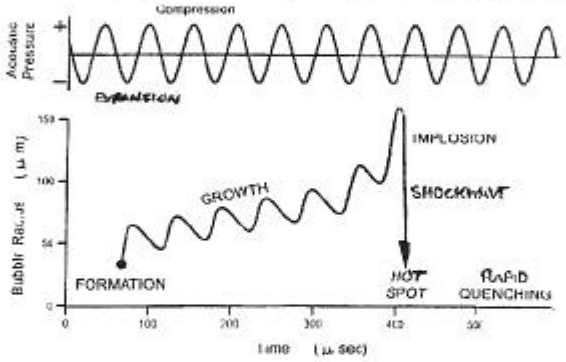

FIG 7 Transient cavitation.

Ultrasound can be added to liquids as shown in Fig. 8. Figure 9 shows the sonoluminescence created by the titanium horn tip of a titanium horn. The temperature created in the hot spots that cause the sonoluminescence is estimated to be about 5000 K. In addition, ultrasound has recently been found to cause many possible chemical effects, including vast improvements in both stoichiometric and catalytic reactions [8]. Intense radiation by ultrasound has been found to increase reactivity by almost one million times. [8]

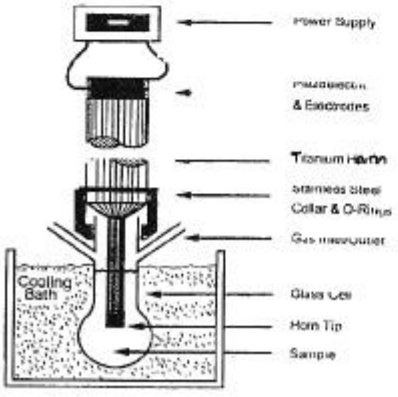

FIG 8 Sonochemical apparatus.

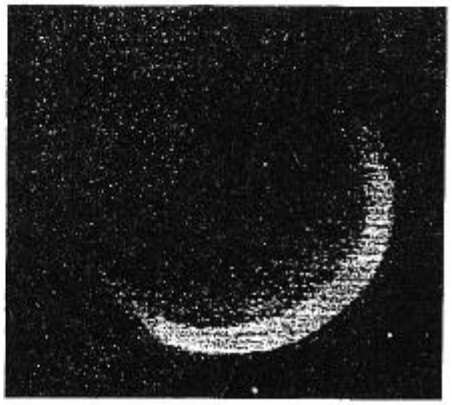

FIG. 9 Sonoluminescence from a Vibrating Tibanium Rod (1 cm long).

THERMOACOUSTIC ENGINES

Thermoacoustic engines have recently been shown to be commercially feasible. Such engines use the thermal effects present in sound waves to produce useful acoustic power from the heat inputs or refrigeration from acoustic power. Swift has given good recent reviews of thermoacoustic engines. [9]

The earliest thermoacoustic engine was the Sondhauss tube shown in Fig 10a. Glassblowers in the 19th Century were aware that when a hot glass bulb was being blown on a cool glass tubular section that sound would sometimes be radiated from the stem tip. The Sondhauss tube is a thermoacoustic prime mover and converts heat into mechanical work in the form of sound. It utilizes an acoustic standing wave with the bulb and stem forming a resonator. Figure 8b shows another example of a standing wave thermoacoustic engine, in this case a thermoacoustic refrigerator. The particular refrigerator shown in Fig 10b has a helium-filled resonator driven by a loudspeaker and containing a stack whose hot heat exchanger is fixed at room temperature. Hofler demonstrated that when this device has a static pressure of 1 MPa and is driven with an amplitude of 30 kPa, its cold heat exchanger reaches a temperature of 200 K. At somewhat higher temperatures it produces 3 W of cooling power with a Carnot efficiency of 0.12. Figure 10c shows a travelling wave thermoacoustic heat pump.

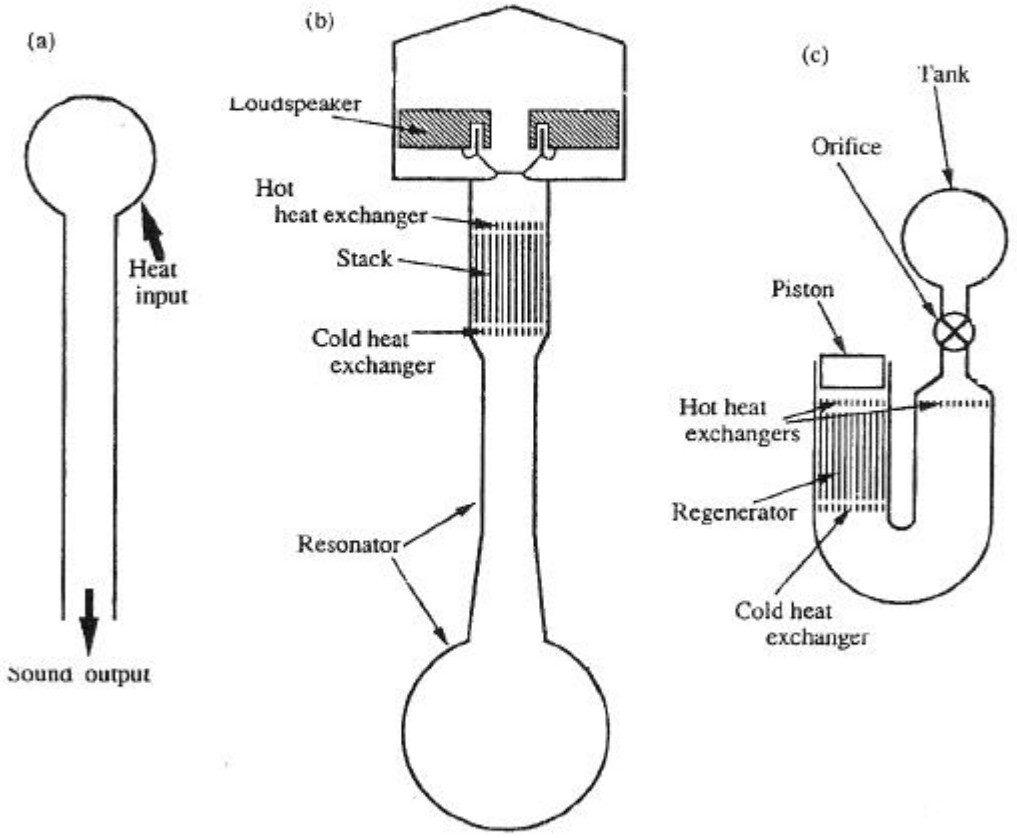

FIG 10 Examples of thermoacoustic engines: (a) the Sondhauss tube, a standing-wave thermoacoustic prime mover; (b) Hofler's refrigerator, a standing-wave thermoacoustic heat pump; (c) the orifice pulse-tube refrigerator, a traveling- wave thermoacoustic heat pump.

A major milestone occurred at Los Alamos in March 1997 when a thermoacoustic refrigerator was used to liquefy natural gas at the rate of 100 gallons a day. This device burned some of the natural gas as a heat source and had a cooling power of 1515 watts and a Carnot efficiency of 19%. The liquefaction was achieved at 115 K (-250 F) and at atmospheric pressure. [10] The advantage of such devices is simplicity of design and maintenance since there are no moving parts. This is a great advantage in liquefying natural gas in field conditions. Further development is underway.

ACTIVE NOISE AND VIBRATION CONTROL

Passive control of noise and vibration can often be achieved through the use of sound absorption, machine enclosure, acoustic barriers, vibration isolation, vibration damping , etc. However all of these measures normally are ineffective at low frequency. Fortunately this is the frequency region in which active control is easiest to implement successfully. The concept has been known for many years. Lueg patented an elementary device for noise control in 1932. However, although there have been quite active research efforts for over 20 years, it is only in the last few years that active control has become commercialized in a few, mostly high technology applications. These include the low frequency exhaust muffling of some internal combustion engines, active vibration isolation of machinery such as automobile engines from vehicle bodies, and the active control of the pure tone propeller noise in the cabins of some light and moderate size passenger aircraft. Recently Nelson and Elliott have given a recent review of active noise control [1] and Fuller of active vibration control. [12]
The advances in active noise and vibration control have become possible for several reasons, but the most important include the recent advances in fast digital signal processing (DSP) computer chips and active control algorithms. In active noise and vibration control systems, secondary inputs are supplied to the system to be controlled in order to modify its response in some desired way. Figures 11 and 12 give an illustration of these with the active control of plane wave sound propagating in a duct. In Fig 11, with feedback control, the error microphone senses the sound signal which is then processed by the controller to produce a suitable control signal for the actuator which attempts to minimize the signal from the error microphone. In Fig 12, with feedforward control, the sound signal is sensed close to the source which is filtered by the electronic controller to produce the desired control signal fed to the actuator (a loudspeaker in this case). The controller attempts to minimize the signal measured by an error sensor (a microphone) using a control algorithm so that the error is minimized.

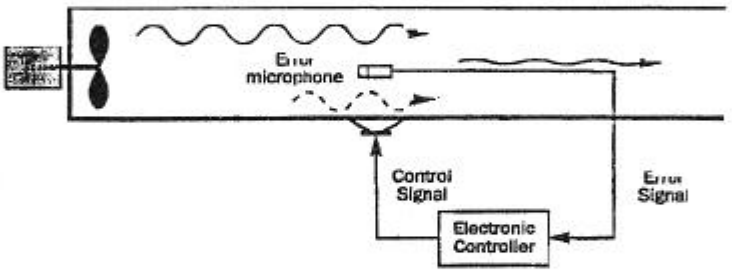

FIG 11 Basic active noise control system. Feedback system

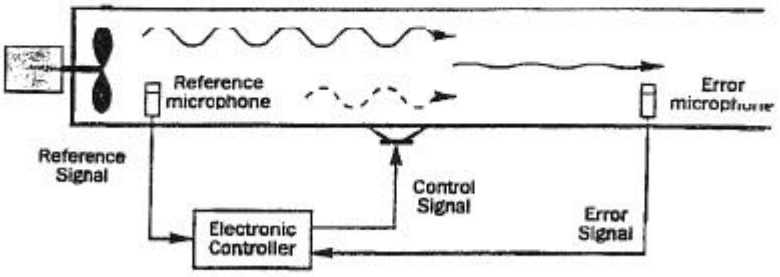

FIG 12 Basic active noise system. Feedforward system

Usually control is implemented digitally using a DSP chip, since in many cases analog circuitry is not practical. (An exception to this is the active hearing protector which normally uses analog control). In the active hearing protector the wavelength is always greater than the earcup cavity dimensions and the error microphone and the noise control source can be collocated in the earcup. Since the passive noise protection of the earcup is normally adequate in the medium to high frequency range above about 1000 Hz, the active protection is only required in the low frequency range below that frequency. Figure 13 shows the noise attenuation of a typical commercial active hearing protector.

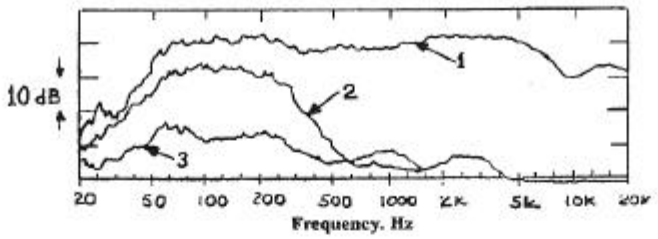

FIG 13 Attenuation provided by typical active hearing protector
1. Sound pressure level at ear of dummy head (no hearing protector)
2. Sound pressure level at ear of dummy head (with passive hearing protector)
3. Sound pressure level at ear of dummy head (with active hearing protector)

In the last five years considerable progress has been made to control the noise in the cabins of commercial aircraft using active control. The noise levels in many civilian turboprop aircraft and rotorcraft are uncomfortably high for the passengers and crew. The noise is dominated by the low frequency, pure tone, blade passing frequency (and multiples) of the propellers or rotor. This noise is transmitted through the cabin side walls to the cabin occupants. Reduction of this sound transmission by passive means is limited by weight restrictions. Active noise control is particularly attractive because pure tone noise is most easily controlled by this technology. Active noise control technology has been applied to a few production turboprop passenger aircraft in the last few years including the SAAB 2000, the SAAB 340B*plus*, and the ATR 42-500 So far the approach has been to use feedforward control with loudspeakers in the cabin wall trim as the control actuators and error microphones in the cabin. The reference signals are obtained from synchronization signals taken from the propeller shafts. This approach has proved quite successful and cabin noise reductions of the order of 10 dB have been achieved. Figure 14a gives an example of the spectrum of the interior cabin noise. The blade passing frequency (BPF) is seen to be of the order of 85 Hz. Figure 14b shows the average cabin sound pressure levels with different numbers of active control loudspeakers in use. The amount of noise reduction achieved depends on the number of loudspeakers used. More recently another active noise control system has been implemented on the de Havilland DASH-8 aircraft range. This system controls the cabin noise by active tuned vibration attenuators (ATVAs) which are attached to fuselage frames in the region around the propeller plane. The ATVAs provide forces to the frames to oppose the fuselage deflections caused by the propeller excitation. Another recent approach that has been investigated involves the reduction of cabin noise by control and minimization of the vibration of the fuselage skin and/or the cabin trim panels. In such an approach, the fuselage wall or cabin trim panel vibration is sensed with PVDF sensors and after processing such signals with a controller, these are fed back to PZT actuators. In some laboratory experiments, reductions in the sound transmission through the walls and panels of over 10 dB have been achieved.

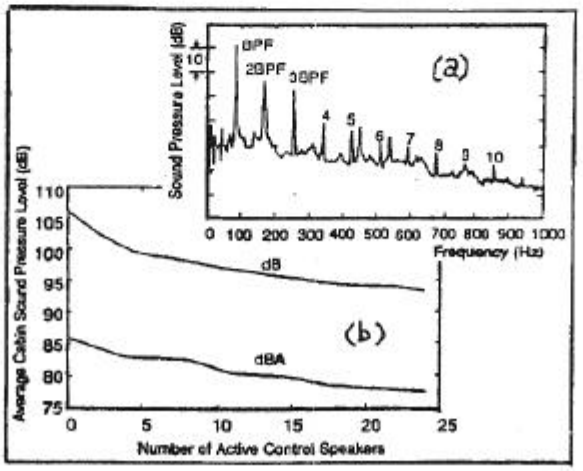

FIG 14 A typical interior noise spectrum of a Saab 340 propeller aircraft and average cabin sound levels with different numbers of active control speakers. The amount of achievable reduction increases with the number of speakers.

SOUND INTENSITY MEASUREMENTS

Sound intensity is a measure of the magnitude and direction of the flow of sound energy. Sound intensity measurements seem to be most useful for the determination of the sound power of large machinery in situ, for noise source identification and for the transmission loss of partitions. [13,14] Care must be taken to sample the sound field appropriately in order to reduce errors. Calibration should be undertaken as recommended by the manufacturers and standards bodies. Crocker and Jacobsen have given a recent review of sound intensity measurements [15].

Figure 15 shows how the sound power of a source can be measured. The sound power of the source is given by the integral of the product of the outgoing sound intensity I_n and the elemental control surface area dS over a measurement surface S enclosing the source. One great advantage of this approach to sound power determination is that sources *extraneous* to the control surface S do not affect the estimate of the sound power. This is because, provided that there is no sound absorbing material inside the control surface S, extraneous sound intensity that enters the surface also leaves it again and the errors cancel out. Since a perfect integration of $I_n dS$ over the surface S cannot be made in practice, either the integral is made by measuring I_n at a number of fixed points or obtaining the surface average of $I_n\, dS$ by moving the sound intensity probe at a steady speed (called scanning) over the measurement surface as illustrated in Fig 16.

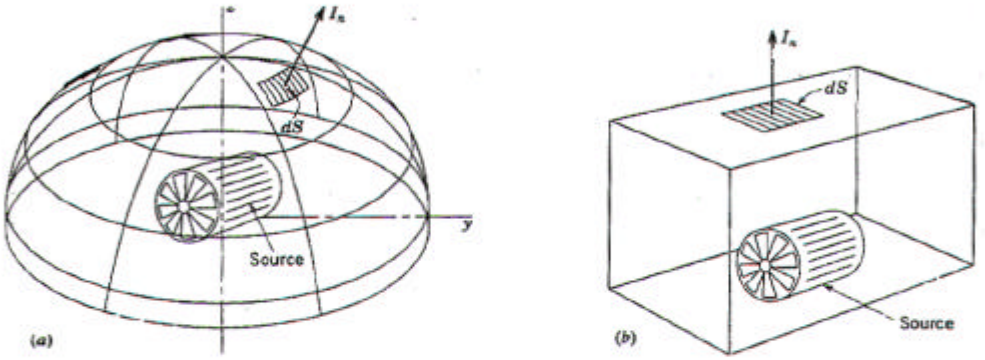

FIG 15 Sound intensity measured on a segment of (a) a hemispherical measurement surface and (b) a rectangular measurement surface.

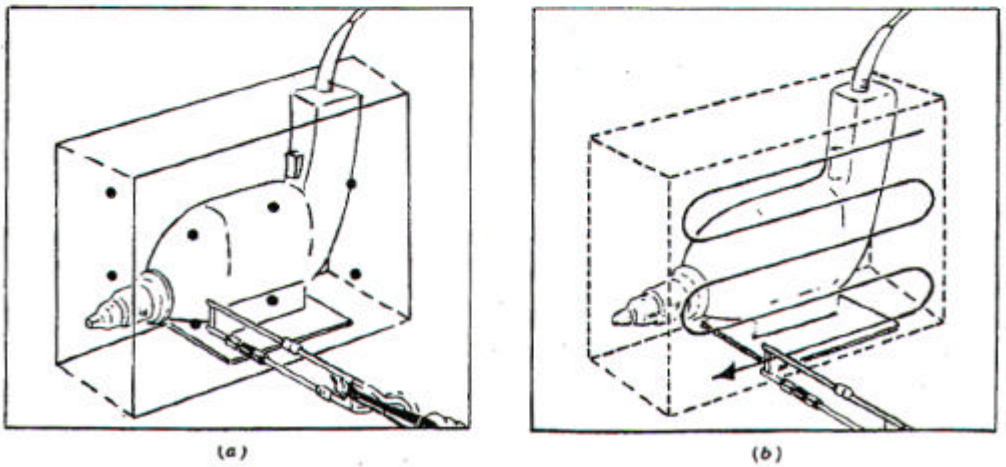

FIG 16 Typical box surface used in sound power determination with the intensity method: (a) measurements at discrete points and (b) measurement path used in scanning measurement

Figure 17 shows the sound power of one part of a diesel engine obtained using the scanning approach. [15] The sound power of the oil pan (sump) of this engine was found to be the dominant noise source responsible for radiating half of the engine sound power. Vector plots of the sound intensity can also be useful in helping

to identify the main noise sources in machinery. The transmission loss (sound reduction index) of a partition can more easily be determined using sound intensity without the use of special facilities since a transmission suite is no longer needed (see Fig 18) and this approach also gives information about the transmission loss (TL) of individual parts of a composite panel such as the one in Fig 19 which is made of aluminium with a Plexiglas (perspex) window. [14,15] The measurement of the sound power of sources using sound intensity measurements has been standardized by ISO, IEC, ANSI and other standards bodies and organizations. [15].

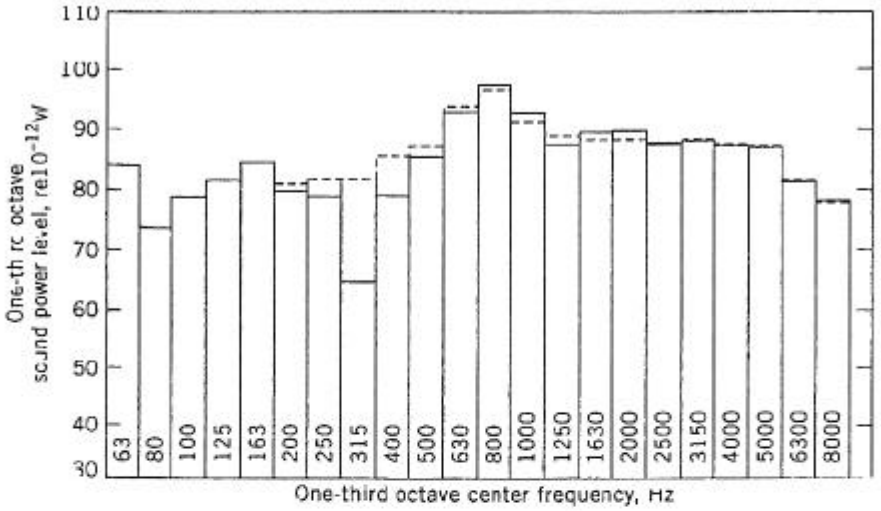

FIG. 17 The sound power of the oil pan of a diesel engine: —, sound intensity method; - - -, lead-wrapping results. (After Reinhart and Crocker)

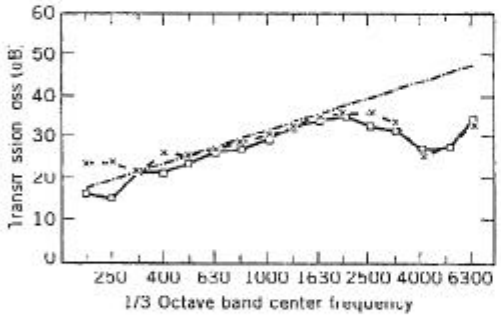

FIG 18 Transmission loss of a 3.2 mm thick aluminum panel: □-□-□, Sound intensity method; x- -x, convention method; – . – . –, mass law. (After Crocker et al.)

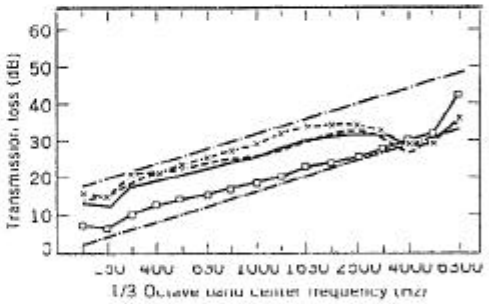

FIG 19 Measured and Calculated transmission loss of a composite aluminum-plexiglass panel. Measured values: x- -x, aluminum; □-□-□, plexiglass; - - -, total transmission loss. Calculate values: –, – , –, mass law, aluminum; -.-.-, mass law, plexiglass; —— total transmission loss (After Crocker et al.)

SPEECH SYNTHESIS AND RECOGNITION

The goal of designing a machine to recognize normal speech, understand it, and respond to it as a human does has not yet been fully achieved. However great strides have been made towards this goal in recent years. Flanagan has recently reviewed the field of speech synthesis and speech recognition. [16]

Speech Synthesis

In the ideal situation we should like a machine to synthesize the equivalent of spoken words from a printed text without any restriction on word vocabulary. This process is normally referred to as text-to-speech

synthesis and is used in a number of financial systems in banks, insurance companies, etc. A system as in Fig 20 is commonly used. With the increased dictionary storage and computing power that recent improvements in digital computers have brought, improvements in speech synthesis have been apparent. The intelligibility of unrestricted text synthesis is quite good, but the speech currently often sounds artificial. Topics of current research include: 1) making the synthesis sound more natural, 2) synthesizing speech with a variety of accents and characteristics including personalizing the speech to represent individual voices, and 3) synthesizing speech in a variety of languages. [16]

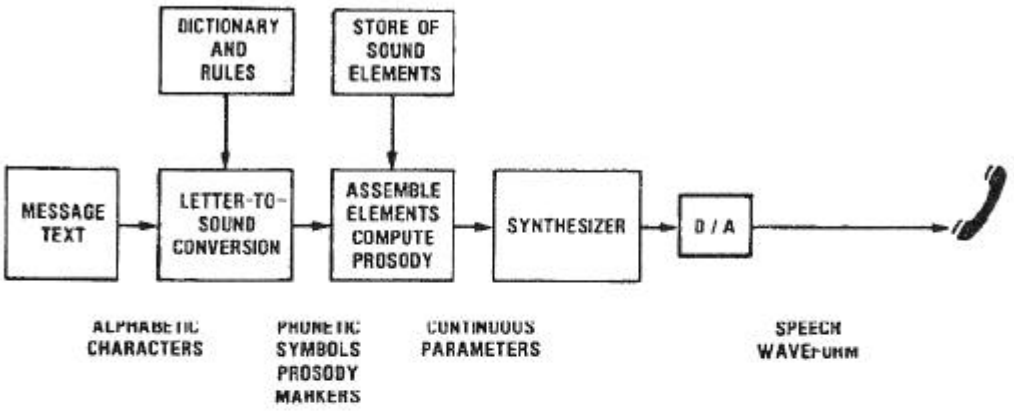

FIG 20 Machine conversion of unrestricted printed text into natural-sounding speech requires transformation of the grapheme (alphabetic character) string into a phonetic equivalent, an understanding of the rules of language for the correct pronunciation of sounds and for voice inflection (pitch, intensity, and duration of sucessive sounds), and a means for controlling an electronic artificial vocal tract to yield an approximation to human speech.

Speech Recognition

Speech recognition is often used to provide access to machines or other systems via voice commands. The user normally speaks to (or commands) a machine. Currently there are three levels of speech recognition: 1) isolated word (or phrase) recognition in which the machine is taught or learns individual words (or phrases) and responds appropriately when these are spoken, 2) recognition of connected words where the machine learns a limited vocabulary of words and responds to a connected string of such spoken words from this vocabulary. (An example is a connected string of spoken digits in applications such as credit card validation, telephone dialing, menu-based access to information, etc.), and 3) continuous speech recognition in which the machine l earns a vocabulary of basic speech units (or sub-words) from which any spoken word can be created by using a sequence of sub-word units and use of a stored dictionary. This third level of speech recognition is often subdivided into: a) *transcription-like systems* (in which every word is recognized uniquely) and b) *spoken language understanding systems* (in which the speech, after recognition, is converted into a natural language question that need not correspond word-for-word with the recognized speech.) [16]

The technology is now well established for very reliable recognition of individual words and phrases selected from vocabularies of limited size. The normal procedure is to use a library of digitally-stored «templates» (containing short-time amplitude spectra of allowed commands) for comparison with the words or phrases uttered. An input command is measured and its spectrum is compared with the spectra of all of the stored library entries. (See Fig. 21). The comparison is normally made using an automatic time-alignment procedure, known as a *dynamic time warp*. The closest fitting template in the library is chosen and the recognized word or phrase is normally repeated to the user using the machine's synthetic voice. The user is asked to confirm that the word or phrase has been correctly recognized. Some speech recognition systems are designed to recognize speech and differentiate between the different individuals and recognize them. A system for talker verification is shown in Fig. 22.

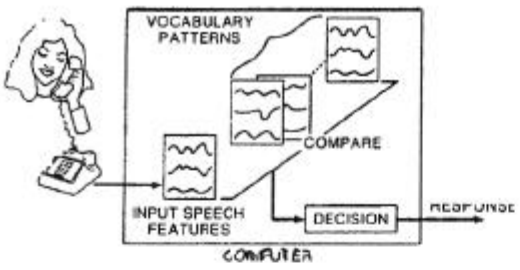

FIG 21 Automatic speech recognition requires comparison of acoustic features measured for an unknown input with stored templates or statistical models for vocabulary items acceptable by the machine. The stored parameters describe short-time spectral characteristics of the vocabulary entries.

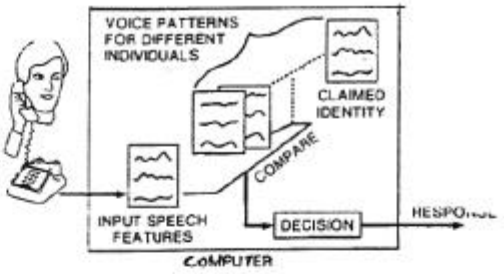

FIG. 22 Talker verification systems perform authentication of a claimed identity through measurements on the voice signal and comparison to a stored pattern known to characterize the claimed individual. A preassigned confidential code phase adds to the security. The machine measures the voice input, makes the comparison, and decides whether to accept or reject the identity claim.

ACOUSTICAL MEDICAL INSTRUMENTATION AND MEASUREMENTS

The use of ultrasound in medicine has had an increasing role in the last twenty years. It is used for several purposes including: 1) therapeutic heating, 2) surgical purposes, 3) passive analysis of heart and lung sounds for diagnosis, and 4) medical imaging. Greenleaf has written a recent review of acoustical medical instrumentation. [17] Ultrasound is used for therapeutic heating, because unlike electromagnetic radiation, it combines a relatively great depth of penetration with a relatively short wavelength. It is thus possible to ensure that deep heating occurs in the localized tissues desired for treatment. The heat produced by the ultrasonic wave per unit volume is proportional to the negative divergence of the sound intensity in the wave. [17]

Recently Ultrasonic Doppler Flowmetry has been used to detect and analyze blood flow. [17] For ultrasonic medical imaging and other related diagnostic applications, short wavelengths allow high resolution pictures of structures deep inside the body to be obtained. The use of ultrasonic medical imaging continues to grow because of the availability of real-time imaging, Doppler blood flow measurements, new transducer design, better signal processing, miniaturization and computerization of electronics, lack of x-ray radiation and exposure, and the high information/cost ratios of the images obtained. The medical fields of cardiology, obstetrics, gynecology, and other areas of medicine have been greatly impacted and advanced by the use of ultrasonic imaging technology. [17]

The transducer used must couple directly onto human tissue and must convert an electrical voltage pulse of several hundred volts into a sound pressure pulse in the tissue and then in a few microseconds receive the weak echoes that produce only a few microvolts of signal. Ceramic materials including lead zirconate-titanate, modified lead titanate and lead metaniobate are the most commonly used transducer materials. Transducers are normally made from composites of PZT rods based in a polymer matrix such as PVDF to obtain better transducer properties and impedance matching with the tissue. (See Fig. 23) [17] Different transducer geometries are possible but the principal ones are rectangular (linear arrays) and circular. A typical ultrasonic medical imaging system is shown in Fig 24. [17]

The transducer transmits a short pulse of ultrasonic waves into the tissue. Then it receives reflected waves that are in turn converted into an electrical signal. An ultrasonic beam is formed in both the transmission and reception phases of the process.

The beam forming is done either 1) physically with lenses or curved transducer elements or 2) electronically. Electronic beam forming in the transmission phase is carried out by sending phased pulses from the elements of the transducer array to produce a beam focused at some chosen depth. In the reception phase, electronic beam forming is accomplished by individually amplifying, delaying and then summing the signals received by the transducer elements. The reflected signals thus received are processed to produce images of the scattering tissue or alternatively to obtain Doppler frequency shifts that indicate blood flow. The flow speed, tissue attenuation and other tissue properties must be properly accounted for. The processed information is then displayed in some logical, consistent way for the user. The beam distribution is mapped onto the viewing system. Provision is normally made for the recording of static and dynamic images from the screen and for their storage and subsequent retrieval.

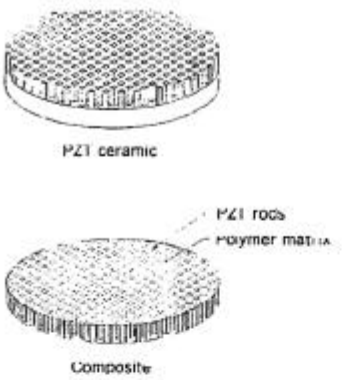

FIG. 23 Composite transducers are made from solid-phase transducers by dicing with a saw and backfilling the kerfs with a polymer. The resulting transducer has low impedance and high coupling constant in addition to physical flexibility. (Reproduced, with permission, from W.A. Smith and A. A. Shaulov, «Composite Piezo electrics: Basic Research to a Practical Device,» Ferroelectrics, Preprint, 1988, pp. 1-12.)

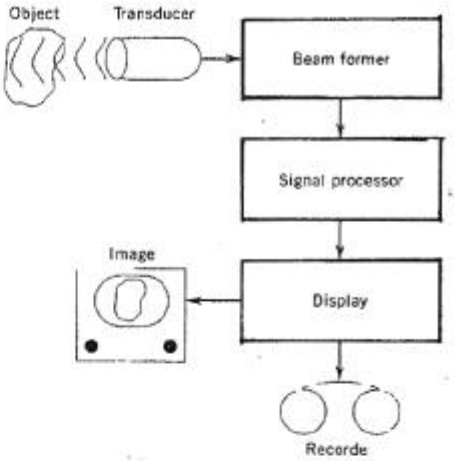

FIG. 24 Principal components of the imaging system are the transducer, the beamformer, the signal processor, the display, and the recorder.

The reflected or scattered sound waves can also be used to detect the fluid motion through the Doppler effect. Doppler shift instrumentation uses either continuous wave or pulsed signals. The signals scattered by the blood cells are processed either in the frequency or the time domain. The relative direction of the beam and of the blood flow must be known if a quantitative knowledge of the flow velocity is desired. Doppler information can be included in B-scan images using colour. The usual convention is to use blue colours to show the flow velocity away from the ultrasonic probe and red to show the flow velocity towards the probe. Often the user will switch the colours to correspond to arterial and venous flow. Turbulence is normally shown in green and the stronger the turbulence the greener the colour. Fig 25 shows a region of the colon with cancer. The cancerous region is the dark area. The image was obtained with a transrectal probe. Rectal probes can also be used to obtain images of the prostate. Fig 26 was obtained with a transvaginal probe. It shows an intrauterine pregnancy. The ovaries can also be imaged using this probe.

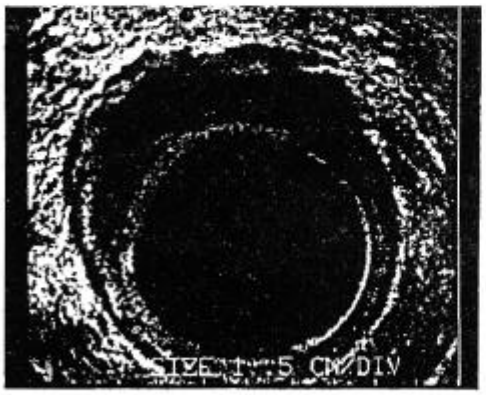

FIG. 25 Image of colon cancer (dark region) obtained from a transrectal ultrasonic probe

FIG. 26 Intrauterine pregnancy imaged by a transvaginal probe.

HEARING AND THE COCHLEA

During the 1970's and 1980's extensive knowledge has been gained into the understanding of the hearing sensitivity of man and other mammals [18]. This was made possible by several new measurement techniques including the implementation of Mossbauer sources. [18] This allowed the «in vivo» determination of the tuning curves for basilar-membrane vibrations near the base of the cochlea for sound levels of over 70 dB. These

results revealed that the cochlea possesses very much greater tuning capabilities than earlier measurements (made on cadavers) had suggested.[18] Further measurements for sound levels of 20 dB or less (made after this technique was refined further) have indicated an even further enormous increase in the sharpness of tuning. This suggests that the sharpness of tuning for the basilar membrane vibrations is similar to the very sharp tuning of the auditory nerve fibres. In the late 1970's Kemp discovered the existence of evoked otoacoustic emissions. [18] As described by Lighthill [18] the analysis of these data suggest that the cochlea performs its well known frequency analysis and obtains its sensitivity to sound at low levels from two main mechanisms. These are:
1) its passive frequency response which occurs because of the steeply graded stiffness variation in the basilar membrane which is immersed in the cochlear fluids. Sound signals at different frequencies become separated from each other with each frequency component completing its passage at its characteristic location on the cochlear at which the local *inner* hair cells generate stimuli that are sent along particular auditory nerve fibres to the cortex.
2) at very low sound levels it has recently been found that there is an active frequency response system related to the *outer* hair cells. These through a process of positive feedback amplify the vibrations of the basilar membrane in a healthy cochlea. This process produces an enhanced signal at low sound levels, so that the threshold at which they can generate activity in the auditory nerve fibres is very much lowered. The *outer* hair cells posses the ability to go into continuous vibration at a particular sound frequency which is sustained by a metabolic power source. Since these vibrations can be stimulated by a very small sound signal they can (on their communication to the basilar membrane) produce a significant enhanced stimulus to the «inner» hair cells.
Figure 27 shows a possible molecular basis for the outer hair cell motor.[18] The area change in the molecule is transformed into a change in cell length. The functioning of the outer hair cells has been recently described by Ashmore and others in a series of papers.[18]

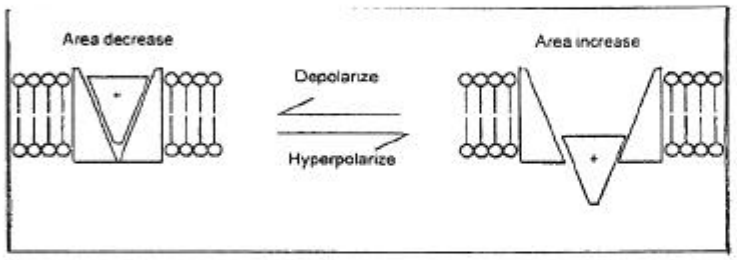

FIG 27
A possible molecular basis for the outer hair cell motor. The molecule is regarded as capable of undergoing a conformation change and as it does so, a charge is transferred across the membrane. Measurement of the total charge transferred gives an estimate of the number of such «particles» present in the membrane. The area change in the molecule is transformed as a change in cell length.

REFERENCES

1. M. Petyt, Introduction to Finite Element Analysis, Cambridge University Press, 1990, Cambridge
2. A. Craggs, Acoustic Modeling: Finite Element Method, Chapter 14 in Encyclopedia of Acoustics, M. J. Crocker (Ed), John Wiley & Sons, New York, 1997.
3. C .I J. Young and M. J. Crocker, Finite Element Acoustical Analysis of Complex Muffler Systems with and without Wall Vibrations, *Noise Control Engineering Journal*, Vol. 9, No. 2, 1977, pp. 86-93.
4. A. F. Seybert and T. W. Wu, Acoustic Modeling: Boundary Element Methods, Chapter 15 in Encyclopedia of Acoustics, M. J. Crocker (Ed), John Wiley & Sons, New York, 1997
5. M. A. Hamadi, Recent Advances in Vibro-Acoustic Computation, Noise-Con 97, Penn State, PA, 1997
6. G. M. Lilley, X. Zhang and A. Rona, Progress in Computational Aeroacoustics in Predicting the Noise Radiated from Turbulent Flows, *International Journal of Acoustics and Vibration*, Vol. 2, No. 1, 1997, pp. 3-10.
7. S. C. Borgowda, U. S. Shirahatti, A. Klotchov and M. J. Crocker, Computational Aeroacoustic Analysis of Ducts, *Proc. Third International Congress on Air- and Structure-borne Sound and Vibration*, Montreal, Canada, pp. 1256-61, 1994
8. K. S. Suslick and L. E. Crum, Sonochemistry and Sonoluminescence, Chapter 26 in Encyclopedia of Acoustics, M. J. Crocker (Ed), John Wiley & Sons, New York, 1997.
9. G. W. Swift, Thermoacoustic Engines, Chapter 61 in Encyclopedia of Acoustics, M. J. Crocker (Ed), John Wiley & Sons, New York , 1997.
10. G. W. Swift, Thermoacoustic Natural Gas Liquifier, *DOE Naturol Gas Conference, Houston, TX*, pp. 1-4, March 1997.
11. P. A. Nelson and S. J. Elliott, Active Noise Control, Chapter 84 in Encyclopedia of Acoustics, M. J. Crocker (Ed), John Wiley & Sons, 1997.
12. C. R. Fuller, Active Vibration Control, Chapter 75 in Encyclopedia of Acoustics, M. J. Crocker (Ed), John Wiley & Sons ,1997.
13. W. P. Waser and M. J. Crocker, Introduction to the Two-Microphone Cross Spectral Method of Determining Sound Intensity, *Noise Control Eng. Journal*, Vol. 22, pp. 76-85, 1984.
14. M. J. Crocker, Sound Intensity, Chapter 14 in Handbook of Acoustical measurements and Noise Control, C. M. Harris (Ed), Third Ed., 1991.
15. M. J. Crocker and F. Jacobsen, Sound Intensity, Chapter 156 in Encyclopedia of Acoustics, M. J. Crocker (Ed), John Wiley & Sons, New York, 1997.
16. J. L. Flanagan, Introduction (to Speech Recognition), Chapter 124, Encyclopedia of Acoustics, M. J. Crocker (Ed), John Wiley & Sons, New York, 1997.
17. J. F. Greenleaf, Acoustical Medical Imaging Instrumentation, Chapter 144 in Encyclopedia of Acoustics, M. J. Crocker (Ed), John Wiley & Sons, New York, 1997.
18. J. Lighthill, Recent Advances in Interpreting Hearing Sensitivity, *International Journal of Acoustics and Vibration*, Vol. 1, No. 1, pp. 5-9, 1996.